

Alternative Oxidase in Resistance to Biotic Stresses: *Nicotiana attenuata* AOX Contributes to Resistance to a Pathogen and a Piercing-Sucking Insect But Not *Manduca sexta* Larvae^{1[W][OA]}

Lu Zhang, Youngjoo Oh, Hongyu Li, Ian T. Baldwin, and Ivan Galis^{2*}

Department of Molecular Ecology, Max Planck Institute for Chemical Ecology, Jena D-07745, Germany (L.Z., Y.O., I.T.B., I.G.); and School of Life Sciences, Lanzhou University, Lanzhou 730000, People's Republic of China (L.Z., H.L.)

The role of the alternative respiratory pathway in the protection of plants against biotic stress was examined in transgenic tobacco (*Nicotiana attenuata*) plants (irAOX) silenced in the expression of *ALTERNATIVE OXIDASE* (AOX) gene. Wild-type and irAOX plants were independently challenged with (1) chewing herbivores (*Manduca sexta*), (2) piercing-sucking insects (*Empoasca* spp.), and (3) bacterial pathogens (*Pseudomonas syringae* pv *tomato* DC3000), showing that all these treatments can strongly elicit accumulation of AOX gene transcripts in wild-type plants. When *N. attenuata* chemical defenses and resistance were examined, irAOX plants showed wild-type levels of defense-related phytohormones, secondary metabolites, and resistance to *M. sexta*. In contrast, piercing-sucking leafhoppers (*Empoasca* spp.) caused more leaf damage and induced significantly higher salicylic acid levels in irAOX compared with wild-type plants in the field and/or glasshouse. Subsequently, irAOX plants accumulated lower levels of defense metabolites, 17-hydroxygeranylinalool diterpene glycosides, caffeoylputrescine, and nicotine compared with wild-type plants under prolonged attack of *Empoasca* spp. in the glasshouse. Finally, an accelerated cell death phenotype was observed in irAOX plants infected with *P. syringae*, which correlated with higher levels of salicylic acid and hydrogen peroxide levels in pathogen-infected irAOX compared with wild-type leaves. Overall, the AOX-associated changes in phytohormone and/or redox levels appear to support the resistance of *N. attenuata* plants against cell piercing-sucking insects and modulate the progression of cell death in pathogen-infected tissues but are not effective against rapidly feeding specialist herbivore *M. sexta*.

Metabolic plasticity allows plants to adapt to variable environmental stress conditions. Plants rapidly reconfigure their primary metabolism during stress to cope with the increased metabolic demands of resistance responses, and mitochondria are known to play a central role in this reconfiguration (for review, see Bolton, 2009; Millar et al., 2011). Under stress, electrons are frequently rerouted through an alternative respiratory pathway branching from the cytochrome (Cyt) pathway at the level of ubiquinone (UQ) pool to an enzyme known as the alternative oxidase (AOX; McDonald, 2008). In contrast with the Cyt pathway, the AOX pathway is resistant to cyanide and therefore known as cyanide-resistant respiration (Henry and Nyns, 1975). The alternative pathway bypasses two important energy

conservation sites (complex III and IV) and avoids oxidative phosphorylation and ATP synthesis: energy is dissipated as heat after reduction of oxygen to water by AOX enzyme (Moore et al., 1978). Whereas alternative respiration is widespread in plants, fungi, and some prokaryotes (McDonald, 2008), its physiological function and seemingly energy-wasting character are not well understood.

One of the most-investigated functions of AOX is heat production, which can volatilize odoriferous compounds during flowering for the attraction of pollinators in Arum lily (*Sauromatum guttatum*) flowers, for example (Meeuse, 1975; Raskin et al., 1987). Heat production is only associated with a limited number of thermogenic plant species (Seymour, 1997), and alternative functions of AOX have been extensively investigated. Subsequently, AOX has been established as one of the essential defense components in plant response to acute stress (Arnholdt-Schmitt et al., 2006). Abiotic stresses such as drought (Bartoli et al., 2005), high salt (Costa et al., 2007; Feng et al., 2010a), low temperature (Vanlerberghe and McIntosh, 1992; Popov et al., 2011; Wang et al., 2011), and wounding (Hiser and McIntosh, 1990) are known to stimulate the activity of alternative respiratory pathways or at least increase AOX transcripts and/or protein levels. Phytochrome, phototropin, and cryptochrome photoreceptors have been shown to mediate the light-responsiveness of the *AOX1a* gene in

¹ This work was supported by the Max Planck Society.

² Present address: Institute of Plant Science and Resources, Okayama University, Kurashiki, Okayama 710-0046, Japan.

* Corresponding author; e-mail igalis@ice.mpg.de.

The author responsible for distribution of materials integral to the findings presented in this article in accordance with the policy described in the Instructions for Authors (www.plantphysiol.org) is: Ian T. Baldwin (baldwin@ice.mpg.de).

^[W] The online version of this article contains Web-only data.

^[OA] Open Access articles can be viewed online without a subscription.

www.plantphysiol.org/cgi/doi/10.1104/pp.112.200865

Arabidopsis (*Arabidopsis thaliana*) seedlings, and *aox1a* mutants showed increased photobleaching damage under high light conditions (Zhang et al., 2010). Several studies have indicated that AOX may also function in resistance to biotic stress such as infection by pathogens. For example, AOX protein levels increased in local and systemic *Nicotiana tabacum*, and in tomato (*Solanum lycopersicum*) leaves infected with tobacco mosaic virus (TMV; Lennon et al., 1997; Liao et al., 2012). The over-expression of AOX protein resulted in smaller hypersensitive response lesions, suggesting that AOX may act as a suppressor of programmed cell death (PCD) in virus-infected leaves (Ordog et al., 2002). The induction of AOX in leafy mustard (*Brassica juncea*) during infection with turnip mosaic virus was suppressed in the presence of ethylene biosynthesis inhibitor aminoethoxyvinylglycine, suggesting that ethylene and AOX are likely involved in leafy mustard's systemic resistance to virus infection (Zhu et al., 2011).

Bacterial pathogens and their elicitors also strongly elicit AOX transcript accumulations and protein levels, both in leaves and cell suspensions (Krause and Durner, 2004; Mizuno et al., 2005; Kiba et al., 2008). In *Arabidopsis* plants, infection with virulent and avirulent strains of *Pseudomonas syringae* pv *tomato* (*Pst*) elevated AOX transcript and protein levels in infected leaves (Simons et al., 1999). An accurate oxygen isotope discrimination method was used to determine the partitioning of electrons between Cyt and the alternative pathways in pathogen-infected plants and documented a 5-fold increase in in vivo AOX activity 4 h after application of the bacterial elicitor harpin N_{Ea} to *Nicotiana sylvestris* leaves (Vidal et al., 2007). In *Paracoccidioides brasiliensis*, a human thermal dimorphic pathogenic fungus, PbAOX played an important role in fungal defense response against oxidative stress imposed by immune cells and virulence of the pathogen (Ruiz et al., 2011).

Therefore, control of oxidative damage is essential for living organisms, including plants, to survive under and recover from stresses (Hanqing et al., 2010). Here, AOX is very likely to counteract the overreduction of mitochondrial UQ pools by consuming excess reducing equivalents, particularly when the flow of electrons through the Cyt pathway is impaired by acute stress. Because insects and microbial attacks are both knowingly associated with oxidative bursts (Torres et al., 2002; De Vos et al., 2007; Maffei et al., 2007), AOX and its redox-controlling function could contribute to a plant's resistance to herbivores and pathogens. To test this expectation, we transformed *Nicotiana attenuata* plants with an RNA interference (RNAi) construct harboring a fragment of *NaAOX* gene in an inverted repeat orientation (irAOX) to silence the expression of endogenous *NaAOX* genes and selected three mechanistically distinct biotic stress models to thoroughly examine the role of AOX in plant defense against biotic stresses. Whereas *NaAOX* transcript and protein levels significantly increased in response to all three stress conditions, AOX played different roles in response of plants to these different biotic stresses.

RESULTS

Identification of AOX Gene Sequences in *N. attenuata*

Two AOX genes, *NaAOX1* and *NaAOX2*, from *N. attenuata* of nearly identical nucleotide sequence, have been previously deposited in public National Center for Biotechnology Information databases (AY422688, AY422689). Both genes show a high level of identity to members of the *Arabidopsis AOX1* gene family: *NaAOX1* and *NaAOX2* proteins are 70.7% and 70.3% identical to *AtAOX1a* from *Arabidopsis* (Supplemental Fig. S1A). The high degree of identity between *NaAOX1* and *NaAOX2* genes at the nucleotide level did not allow for efficient monitoring and gene-specific silencing of individual *NaAOX* isoforms by quantitative reverse transcription PCR (qRT-PCR) and RNAi, respectively. Therefore, primers detecting transcripts of both genes were used and reported herein as *NaAOX* transcript abundance. Subsequently, both genes were targeted with a single silencing construct to down-regulate AOX expression. Despite our attempts to identify additional AOX genes from *N. attenuata*, we were not able to find any additional conserved AOX proteins in this diploid *Nicotiana* species.

Analysis of *NaAOX* Transcript Levels in Response to an Attack from a Chewing Herbivore

Abiotic stress and pathogen elicitors are known to increase transcript levels of AOX genes in plants. However, much less is known about the effects of herbivory. We examined *NaAOX* transcript levels in wild-type leaves subjected to wounding or simulated herbivory treatment, and in *N. attenuata* leaves after direct feeding to *Manduca sexta* neonates. The *NaAOX* transcripts strongly increased 1 h after wounding the *N. attenuata* leaves with a pattern wheel and immediately applying either water to mechanical wounds (W+W) or *M. sexta*'s oral secretions (OS) to simulate herbivory (W+OS; Fig. 1A; Supplemental Fig. S1B). It is interesting that *NaAOX* transcript and protein levels appeared higher in W+OS-compared with W+W-treated leaves at 1 to 3 h (Fig. 1A; Supplemental Fig. S2A). Similarly, direct *M. sexta* feeding significantly elevated basal *NaAOX* transcript and protein levels at 1 and 2 d after placing neonates on the leaves (Fig. 1B; Supplemental Fig. S2B). Because *NaAOX* transcript levels increased significantly more in response to *M. sexta*'s salivary elicitors, we hypothesized that AOX may function in direct defense of *N. attenuata* against chewing herbivores. In addition to the herbivore- and wound-regulated patterns shown in Figure 1, an apparent oscillation in *NaAOX* transcript abundance was observed in untreated control leaves, suggesting a possible circadian control of AOX transcription (Fig. 1A). In particular, AOX transcripts appeared to be higher during the light periods than during dark periods, which could be associated with a previously reported AOX function in buffering high photosynthetic and respiration rates in response to high light (Dinakar et al., 2010).

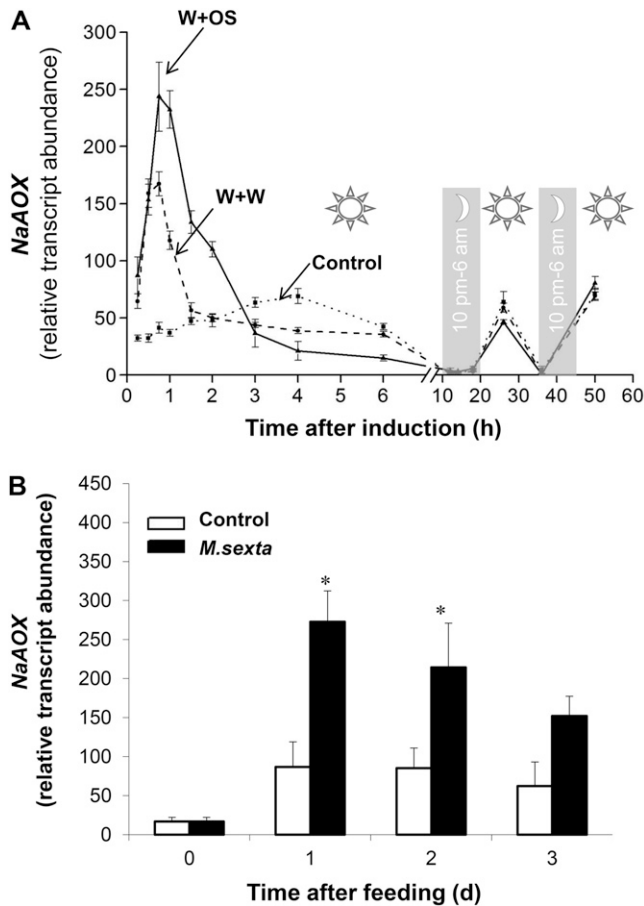


Figure 1. *NaAOX* gene transcripts increase in response to simulated herbivory and feeding of *M. sexta* caterpillars in *N. attenuata*. A, Technical replicate means (\pm SE) of *NaAOX* transcript relative abundances quantified with qRT-PCR in pooled samples using five independent controls, W+W- and W+OS-elicited *N. attenuata* plants. The leaves were elicited with a pattern wheel (wounding) and immediately applying either water to mechanical wounds (W+W) or *M. sexta*'s OS to simulate herbivory (W+OS). Gray areas indicate dark periods showing low *NaAOX* transcript levels. B, Means (\pm SE) of *NaAOX* transcripts quantified with qRT-PCR from control and *M. sexta*-attacked rosette leaves at 0, 1, 2, and 3 d after placing three *M. sexta* neonates on each leaf. Asterisk indicates significant differences between control and insect-fed plants at respective time points (unpaired Student's *t* test, * $P < 0.05$; $n = 3$).

NaAOX Silencing Does Not Compromise Defense of *N. attenuata* against *M. sexta* Caterpillars

To examine the function of *NaAOX* in resistance of *N. attenuata* against its specialist herbivore *M. sexta* caterpillars, we generated stably AOX-silenced *N. attenuata* plants (irAOX) using RNAi and inverted repeat fragment of the *NaAOX1* gene (Supplemental Fig. S3A). Two independent homozygous diploid lines (referred to as irAOX-200 and irAOX-203) carrying a single insertion of transfer DNA were selected for further experiments (Supplemental Fig. S3B). In both lines, the levels of *NaAOX* transcripts were strongly reduced compared with identically treated wild-type plants (Supplemental Fig. S3C). Alternative respiration capacity of the leaves

was also significantly suppressed in irAOX plants compared with wild-type plants (Supplemental Fig. S4).

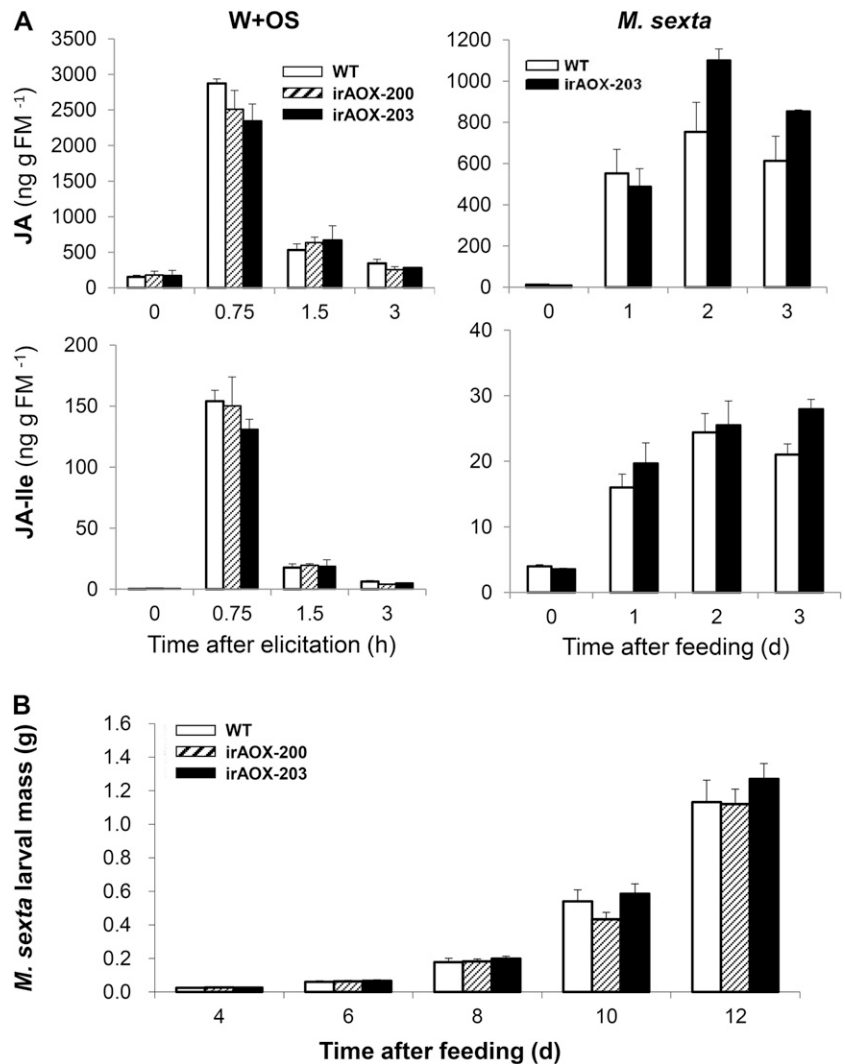
Feeding of *M. sexta* larvae elicits burst of jasmonic acid (JA) and JA-Ile in *N. attenuata* leaves, which triggers defense signaling pathways and deploys defense responses (Wu and Baldwin, 2010). To examine if *NaAOX* mediates changes in phytohormone levels, we determined JA and JA-Ile contents in irAOX and wild-type plants at 0, 45, 90, and 180 min after W+W- and W+OS-elicitation. Similar analysis was conducted using *M. sexta*-attacked leaves before and 1, 2, and 3 d after placing neonates on the leaves. Whereas both treatments elicited significantly higher levels of JA and JA-Ile in the leaves compared with untreated controls, we did not find any significant differences in JA or JA-Ile content between wild-type and irAOX plants (Fig. 2A). The levels of another stress hormone, salicylic acid (SA) remained comparable between wild-type and irAOX plants (Supplemental Fig. S5, A and B) and staining of W+OS and control leaves with 3,3'-diaminobenzidine (DAB) showed comparable levels of hydrogen peroxide (H_2O_2) accumulation in wild-type and irAOX leaves (Supplemental Fig. S5C). Because important defense metabolites such as nicotine (Steppuhn et al., 2004) and 17-hydroxygeranylinalool diterpene glycosides (HGL-DTGs; Jassbi et al., 2008; Heiling et al., 2010) were not differentially regulated in irAOX compared with wild-type plants (Supplemental Fig. S6), it was not surprising that caterpillar performance in feeding bioassays did not differ (Fig. 2B). These results suggest that despite increased transcript levels of *NaAOX* in response to *M. sexta* attack, *NaAOX* genes do not play any significant role in the direct defense of *N. attenuata* plants against chewing specialist herbivores. The induction of *NaAOX* transcripts and protein levels by insect feeding could be a consequence of/and defense against mechanical wounding, similar to previously described accumulation of AOX protein in mechanically wounded potato (*Solanum tuberosum*) tubers (Hiser and McIntosh, 1990).

We also considered an alternative hypothesis that increased AOX expression during herbivory could facilitate higher emissions of volatile organic compounds, mediators of indirect defenses, from herbivore-attacked leaf surfaces of *N. attenuata*. However, in our previous experiments, we did not find any consistent differences in α -bergamotene or benzyl acetone emissions from wild-type and irAOX plants, even when the plants were maintained at less than ambient temperatures (data not shown).

NaAOX Silencing Makes Plants More Susceptible to Piercing-Sucking *Empoasca* spp.

In the natural environment, plants are exposed to a large variety of pests and pathogens. When irAOX-203 plants were transplanted as size-matched pairs with *N. attenuata* wild-type plants into their native habitat in the Great Basin Desert of southwestern Utah, we noticed that leafhoppers (*Empoasca* spp.) caused significantly more damage on irAOX-203 compared with wild-type plants (Fig. 3A). We also observed mirid (*Tupiocoris*

Figure 2. irAOX OS- and herbivory-induced plants have wild-type JA levels and AOX silencing does not affect *M. sexta* caterpillar performance. A, Mean (\pm SE) levels of JA and JA-Ile in samples collected at 0, 0.75, 1.5, and 3 h after wounding and immediately applying OS from *M. sexta* (W+OS; $n = 5$, left), and mean (\pm SE) levels of JA and JA-Ile in samples collected after 0, 1, 2, and 3 d of *M. sexta* feeding ($n = 3$, right). B, Mean (\pm SE) mass of *M. sexta* caterpillars determined after neonates placed on 30 independent wild-type and irAOX plants were allowed to feed for 12 d. No statistically significant differences in caterpillar mass were detected between wild-type and NaAOX gene-silenced lines.



notatus)- and flea beetle (*Epitrix* spp.)-associated damage on the plants in the field; in contrast to *Empoasca* spp. damage, there were no significant differences in damage caused by these insects (data not shown).

The *Empoasca* spp. are cell rupture feeders that are often associated with microbes transmitted during herbivore feeding (Backus et al., 2005). Although *Candidatus* *Phytoplasma* spp. have not been identified in *Empoasca* spp. occurring in the Utah field or in our in-house colony derived from Utah-collected insects (Kallenbach et al., 2012), it suggests that AOX is important for protection of plants against sucking-piercing insects and/or other microbes, such as viruses and bacteria, vectored by these insects. To examine the robustness of our initial field observations, a choice-test experiment with irAOX and wild-type plants was conducted in the glasshouse. An equal number of wild-type and irAOX-203 plants were placed in a randomized design in the sealed glass container with *Empoasca* spp. that were allowed to feed on the plants for 12 d. Consistent with our field observations, irAOX plants were significantly more damaged compared with wild-type plants (Fig. 3B).

The NaAOX transcript and protein levels were determined before and after 4, 8, and 12 d of exposure of wild-type plants to *Empoasca* spp. feeding (Fig. 4; Supplemental Fig. S2C). *Empoasca* spp. feeding induced NaAOX transcripts that became 6-fold more abundant compared with control plants after 12 d of exposure (Fig. 4). The consistently higher damage on attacked irAOX plants (Fig. 3B) and inducible character of NaAOX gene shown in Figure 4 prompted a more detailed analysis of *N. attenuata* phytohormone and defense metabolite profiles after *Empoasca* spp. attack.

irAOX Plants Contain Higher Levels of SA after *Empoasca* spp. Attack

Piercing-sucking insects such as aphids, mites, and leafhoppers can activate both salicylate- and JA-dependent defense signaling pathways in plants (Ament et al., 2004; Mozoruk et al., 2006; Kempema et al., 2007). The lack of AOX activity in irAOX *N. attenuata* plants clearly disturbed the homeostasis of SA after *Empoasca* spp. attack. Although SA levels did not differ in the

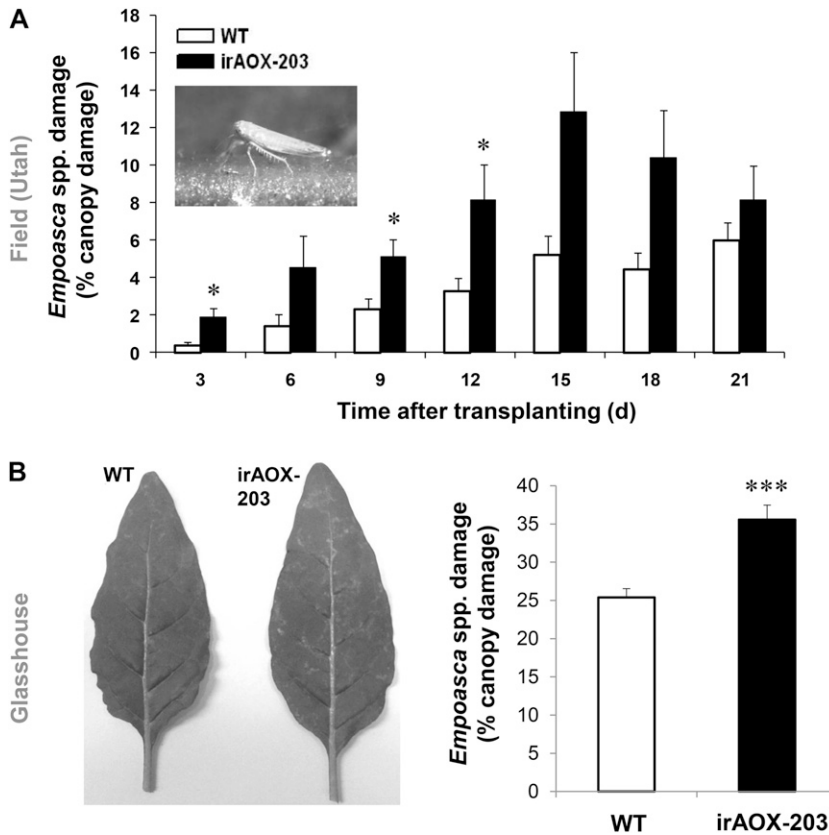


Figure 3. irAOX plants are more susceptible to *Empoasca* spp. damage in the glasshouse and natural environment. A, Mean (\pm SE) average leaf damage by *Empoasca* spp. in wild-type and irAOX plants planted in a pairwise design in the natural environment of *N. attenuata* in the Great Basin Desert ($n = 25$). B, Leaves from wild-type and irAOX plants that were placed for 12 d in a closed cage in the glasshouse with *Empoasca* spp. feeding estimated at the end of the experiment ($n = 10$, right). Asterisk indicates significant differences between wild-type and irAOX plants at respective time points determined by unpaired Student's *t* test (* $P < 0.05$; *** $P < 0.001$). Inset in A, *Empoasca* spp. photographed in the field.

control nonattacked wild-type and irAOX-203 set of plants, SA levels increased in response to *Empoasca* spp. attack in irAOX, but remained unchanged in wild-type plants (Fig. 5A). In contrast, JA and JA-Ile levels were not differentially elicited in wild-type and irAOX plants (Fig. 5B). It is likely that JA levels after *Empoasca* spp. attack increased only transiently and/or locally, which was not captured in our experimental setup (first measurement after 4 d). Recently, a significant increase in JA levels was reported in the leaves of *N. attenuata* challenged with 25 *Empoasca* spp. individuals allowed to feed on the leaf for 2 d (Kallenbach et al., 2012). In addition, reduced resistance to *Empoasca* spp. was found in the field and glasshouse experiments with JA biosynthesis-deficient *N. attenuata* plants (Kessler et al., 2004; Kallenbach et al., 2012). In addition, irLOX3 plants silenced in the accumulation of JA were significantly more damaged by *Empoasca* spp. compared with wild-type plants in our glasshouse choice test experiments (Supplemental Fig. S7), emphasizing a central role for JA in *Empoasca* spp. feeding behavior.

Empoasca spp.-Attacked irAOX Plants Have Attenuated Defense Metabolite Accumulations after Prolonged Feeding

Plants use a large variety of secondary metabolites to defend against herbivores and pathogens (Baldwin 2001; Metlen et al., 2009). Nicotine, caffeoylputrescine (CP), and HGL-DTGs are typical secondary metabolites

found in *N. attenuata* plants elicited with biotic stresses (Steppuhn et al., 2004; Heiling et al., 2010; Kaur et al., 2010). Whereas nicotine and HGL-DTGs are known to strongly inhibit *M. sexta* larvae feeding, hydroxycinnamic acid-polyamine conjugates like CP can function against both herbivores and microbes (for review, see Bassard et al., 2010). In our experiments, nicotine ($P < 0.001$),

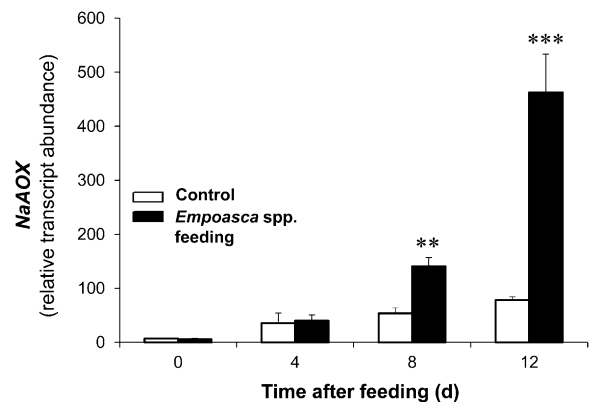
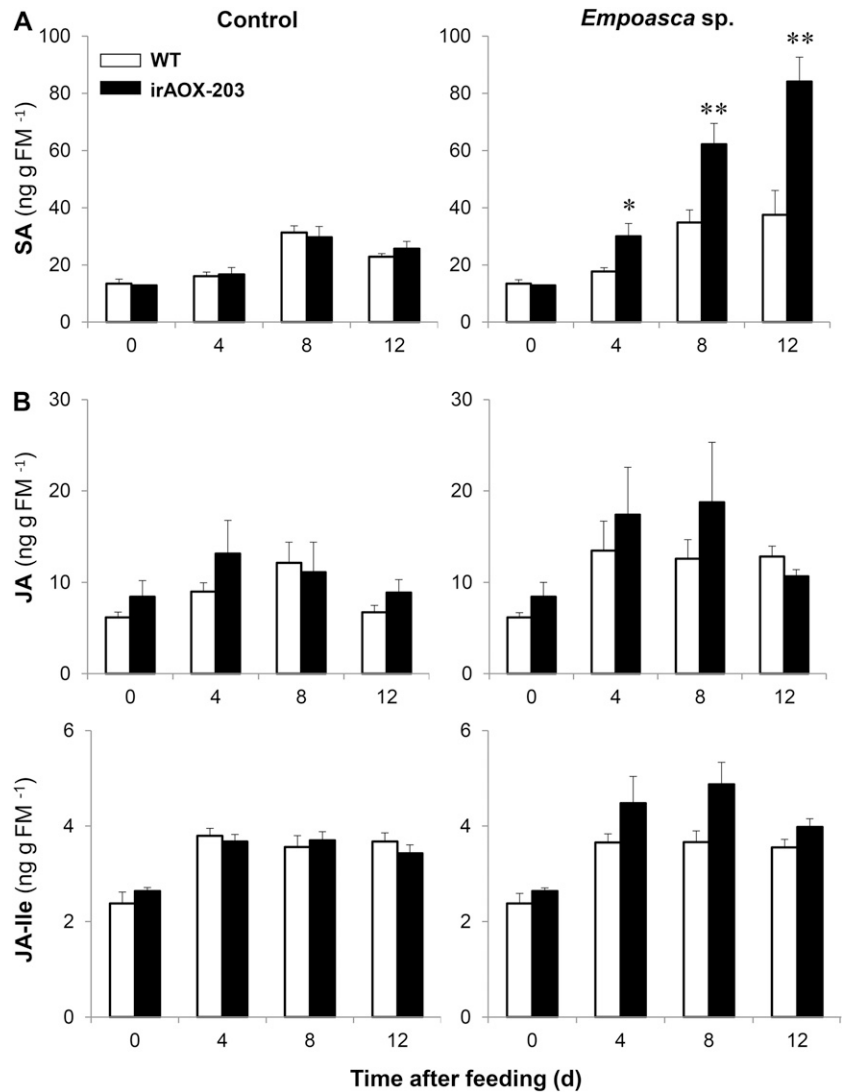


Figure 4. Leaf *NaAOX* gene transcript levels increase in response to *Empoasca* spp. attack. Means (\pm SE) of *NaAOX* relative transcript abundances quantified with qRT-PCR in control and *Empoasca* spp.-attacked wild-type leaves at 0, 4, 8, and 12 d. Asterisk indicates significant differences between control and *Empoasca* spp.-damaged plants at respective time points (unpaired Student's *t* test, ** $P < 0.01$, *** $P < 0.001$; $n = 6$).

Figure 5. Long-term *Empoasca* spp. feeding results in differential SA but not JA levels in irAOX plants. A, Mean (\pm se) levels of SA. B, JA and JA-Ile in samples collected after 0, 4, 8, and 12 d of *Empoasca* spp. feeding. Asterisk indicates significant differences between wild-type and irAOX plants at respective time points determined by unpaired Student's *t* test (* $P < 0.05$, ** $P < 0.01$; $n = 6$).



CP ($P < 0.05$), and HGL-DTGs ($P < 0.001$) accumulated significantly less in irAOX compared with wild-type plants exposed for 8 to 12 d to *Empoasca* spp. feeding (Fig. 6), suggesting a positive role of AOX in efficient accumulation of these metabolites after prolonged *Empoasca* spp. feeding. The initial feeding of *Empoasca* spp., however, is known to be independent of nicotine, HGL-DTGs, and pathogen infections in *N. attenuata* plants (Kallenbach et al., 2012). Consistently, after 4 d of *Empoasca* spp. feeding, defense metabolites were not yet elicited (Fig. 6).

NaAOX Transcripts Increase in Response to Pathogen Infection

The treatment of *N. sylvestris* cells with pathogen-associated elicitors is known to alter partitioning between Cyt- and AOX-dependent respiratory pathways, and transiently increase AOX expression (Vidal et al., 2007). We examined if *Pst* DC3000 strain infection can induce AOX expression in *N. attenuata*;

Pst DC3000 causes local chlorosis followed by leaf necrosis in *N. attenuata* (Hettenhausen et al., 2012). The leaves of rosette stage plants were infiltrated with 1×10^5 colony forming units suspension of *Pst* DC3000, and samples were collected from infiltrated leaf areas before and 45 and 90 min and 3, 24, 48, and 72 h after pathogen inoculation. Both mock- and pathogen-inoculated leaves experienced a transient burst of NaAOX transcripts at 45 min post inoculation (Fig. 7), which was likely caused by wounding during infiltration process. However, transcript and protein levels of NaAOX dramatically up-regulated in pathogen-inoculated compared with mock-treated leaves at the later stages of infection (Fig. 7; Supplemental Fig. S2D), suggesting a direct involvement of AOX in plant defense against pathogen-imposed stress. The levels of NaAOX protein in *Pst*-infected leaves of irAOX-200 and irAOX-203 transgenic lines remained low at 2 and 3 d (Supplemental Fig. S2D), as expected from AOX-silencing efficiency shown in Supplemental Fig. S3C.

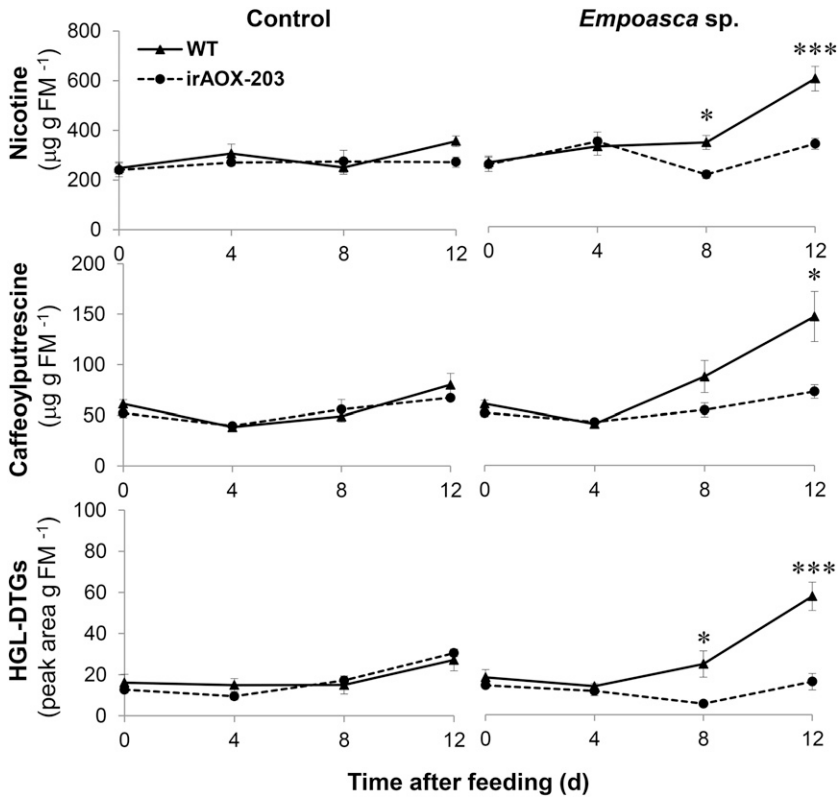


Figure 6. Secondary metabolite levels significantly differ in *Empoasca* spp.-attacked wild-type and irAOX leaves. Mean (\pm SE) levels of defensive secondary metabolites in wild-type and irAOX-203 leaf samples collected after 0, 4, 8, and 12 d of exposure to *Empoasca* spp. Asterisk indicates significant differences between wild-type and irAOX plants at respective time points determined by unpaired Student's *t* test (* P < 0.05, ** P < 0.01, *** P < 0.001; n = 6).

NaAOX Silencing Accelerates *Pst* DC3000-Induced Cell Death

In the following experiment, we observed the progress of necrosis in wild-type and irAOX leaves inoculated with *Pst* DC3000. Both irAOX-200 and irAOX-203 lines exhibited moderately but reproducibly accelerated development of necrotic symptoms, which typically occurred 1 d earlier in irAOX compared with wild-type plants (Fig. 8A, left). Microscopic examination of trypan blue-stained leaves confirmed more extensive cell death in irAOX leaves 2 d after inoculation with the pathogen compared with identically treated wild-type leaves (Fig. 8A, right). When the extent of cell death was estimated by quantitative electrolyte leakage of the cells (Pike et al., 1998), the levels of leakage were significantly higher in both irAOX lines compared with wild-type plants at 24, 48, and 72 h after *Pst* DC3000 infiltration (Fig. 8B).

To characterize *Pst*-induced cell death at a molecular level, the expression of a *N. attenuata* hypersensitive response marker *HAIRPIN-INDUCED1* (*HIN1*) gene was examined. *HIN1* is known to be highly expressed during incompatible plant-pathogen interactions in *N. tabacum* (Takahashi et al., 2004a, 2004b). *NaHIN1* transcripts were significantly induced by *Pst* DC3000 in *N. attenuata*, and they were significantly higher in two irAOX lines compared with wild-type plants 3 d after infection (Fig. 8C). Accelerated cell death process only slightly decelerated bacterial growth in irAOX leaves at 1 (irAOX-200, 203) and 2 (irAOX-203) d after inoculation with the pathogen (Supplemental Fig. S8A).

irAOX Plants Accumulate Higher Levels of H_2O_2 after *Pst* Infection

Cellular reactive oxygen species (ROS) is an important signaling molecule in eukaryotic cells (Rhoads et al., 2006). One of the proposed functions of AOX in

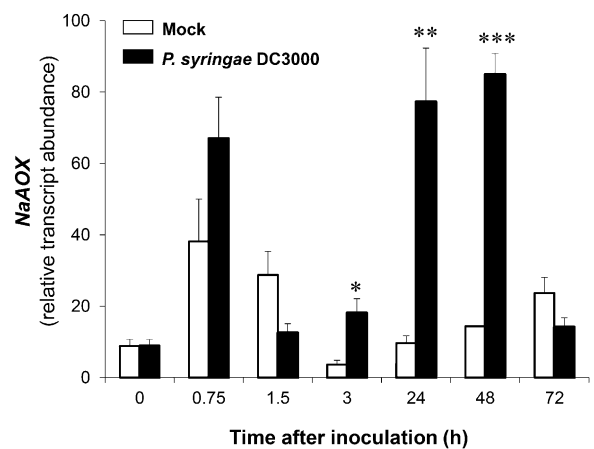


Figure 7. *NaAOX* gene transcripts increase in response to infection with *Pst* DC3000 in *N. attenuata* leaves. Mean (\pm SE) *NaAOX* relative transcript abundances quantified with qRT-PCR in three independent mock- and *Pst* DC3000-inoculated wild-type plants at indicated time points. Asterisk indicates significant differences between mock- and *Pst* DC3000-infected leaves at respective time points determined by unpaired Student's *t* test (* P < 0.05, ** P < 0.01, *** P < 0.001; n = 3).

abiotic stress resistance is the prevention of overreduction of the mitochondrial UQ pool that can counteract the formation of mitochondrial ROS (Maxwell et al., 1999; Umbach et al., 2005).

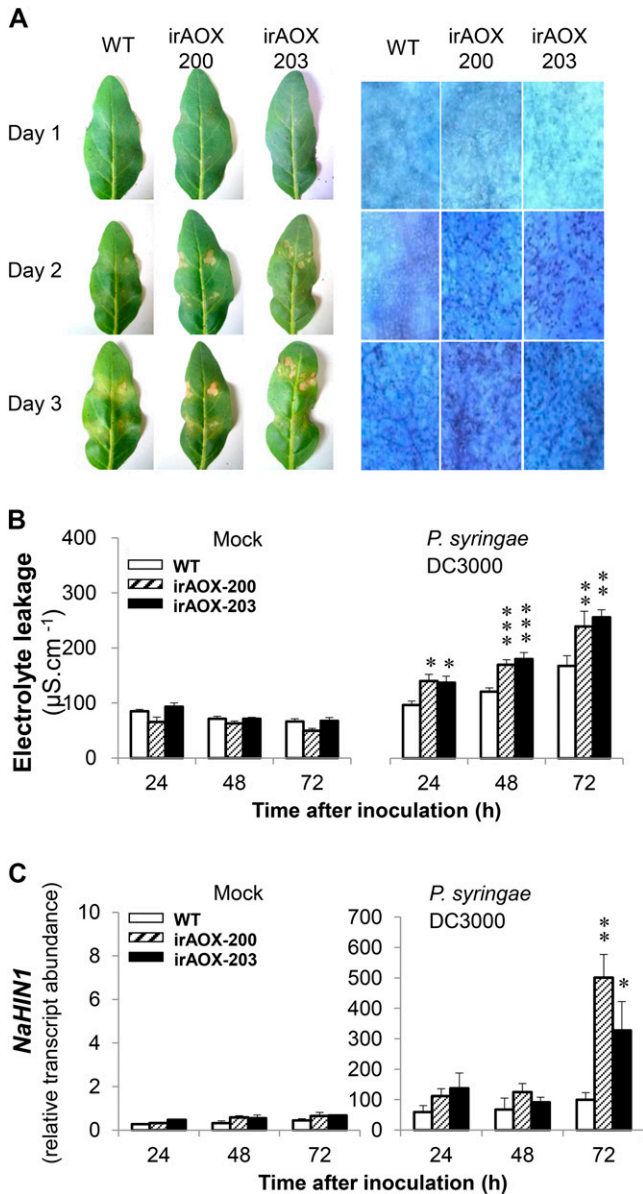


Figure 8. *NaOX* gene silencing accelerates cell death after infection of plants with *Pst* DC3000 pathogen. A, *Pst* DC3000-infected leaves from wild-type and two *irAOX* independent lines (200 and 203) at 1, 2, and 3 d after inoculation (left), and trypan blue-stained leaves at the corresponding time points (right). B, Mean (\pm se) electrolyte leakage from mock and *Pst*-infected leaves in wild-type and two *irAOX* lines determined at 1, 2, and 3 d after inoculation. Significant differences were determined for each time point by one-way ANOVA (* $P < 0.05$, ** $P < 0.01$, *** $P < 0.001$; $n = 5$). C, Mean (\pm se) relative transcript levels of cell death marker gene *NaHIN1* in mock and *Pst* DC3000-inoculated leaves of wild-type and two *irAOX* lines. Significant differences at respective time points were determined by one-way ANOVA (* $P < 0.05$, ** $P < 0.01$; $n = 5$).

We first examined the levels of H_2O_2 by semiquantitative histochemical DAB staining of wild-type and *irAOX* leaves after *Pst* DC3000 infection. A strong brown precipitate of oxidized DAB was observed in both the wild type and two *irAOX* lines at 1 to 3 d after inoculation, but the staining intensity at 2 d appeared stronger in *irAOX* compared with wild-type leaves (Fig. 9A). To determine H_2O_2 contents more precisely, we used sensitive quantitative Amplex red hydrogen peroxide/peroxidase assay kit and determined H_2O_2 levels in the leaves. *Pst* DC3000 infiltration resulted in a strong increase in H_2O_2 content at 2 d post inoculation in both wild-type and *irAOX* plants, and these levels were significantly higher in *irAOX* leaves (Fig. 9B), coinciding with a more rapid development of cell death symptoms in these plants (Fig. 8A).

Previously, the Arabidopsis respiratory burst oxidase homolog D (*RbohD*) was shown to produce a majority of ROS found in pathogen-infected Arabidopsis leaves (Torres et al., 2002). We therefore examined the expression of a putative *NaRbohD* homolog in *N. attenuata* after *Pst* DC3000 inoculation. The transcripts of this *NaRbohD* gene increased both in the wild type and *irAOX* (lines 200 and 203) but appeared significantly higher in *irAOX*-infected leaves (Fig. 9C). This suggests that this *RbohD* homolog may contribute to the higher ROS levels observed in *irAOX* lines, possibly in response to a retrograde mitochondrial signal and/or the accumulation of SA, as proposed below.

SA Levels Increase Significantly More in Pathogen-Infected *irAOX* Leaves

Accumulation of SA is one of the critical features in plant defense against pathogens (for review, see Vlot et al., 2009). As expected, SA levels dramatically increased in both wild-type and *irAOX* plants after *Pst* DC3000 infection, showing maximum accumulations at 24 h in *Pst*-infected wild-type leaves (Fig. 10A). SA levels steadily increased in *irAOX* plants and reached their putative maximum at 72 h, which was 2 times higher compared with SA levels in wild-type plants (Fig. 10A). It is interesting that higher levels of SA in pathogen-infected *irAOX* plants negatively correlated with lower levels of induced JA in these leaves, suggesting a negative cross talk between *Pst* DC3000-induced SA and JA accumulations (Fig. 10A).

In agreement with the higher SA levels, transcripts of two known *PHE AMMONIA-LYASE* (*PAL*) genes in *N. attenuata*, *NaPAL1* and *NaPAL2*, were significantly more induced in *irAOX* compared with wild-type plants, attaining approximately 3-fold higher levels 72 h after inoculation (Fig. 10B). This observation provides a potential explanation for higher accumulation of SA in *irAOX* plants via benzoic acid-dependent SA biosynthetic pathway (Vlot et al., 2009). In contrast to *PAL* expression, the transcripts of isochorismate synthase (Vlot et al., 2009) encoding another SA biosynthetic pathway, although induced by the pathogen, were not

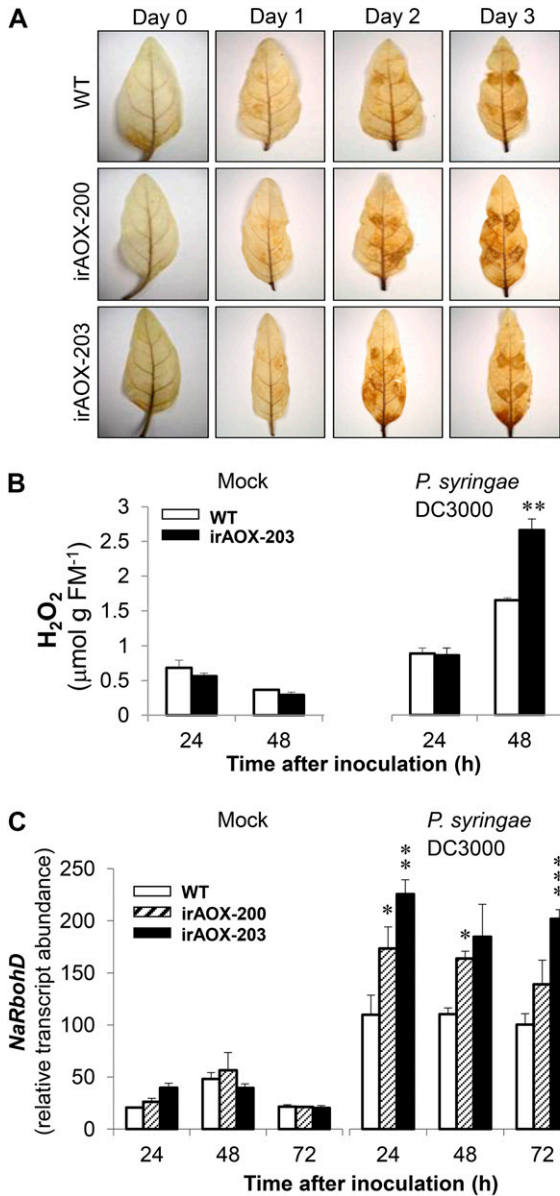


Figure 9. *Pst*-infected leaves of irAOX plants show higher levels of H₂O₂ and increased expression of the *NaRbohD* gene. A, DAB-stained *Pst* DC3000-infected leaves from wild-type and two irAOX lines at 1, 2, and 3 d post inoculation. B, Mean (\pm SE) H₂O₂ levels in mock- and *Pst* DC3000-infected wild-type and irAOX leaves determined at 24 and 48 h post inoculation. Asterisk indicates significant differences between wild-type and irAOX plants at respective time points determined by unpaired Student's *t* test (***P* < 0.01; *n* = 5). C, Mean (\pm SE) of *NaRbohD* relative transcript abundances quantified with qRT-PCR in mock- and *Pst* DC3000-inoculated leaves at indicated time points (*n* = 3). Asterisk shows significant differences between wild-type and irAOX plants at respective time points determined by one-way ANOVA (**P* < 0.05, ***P* < 0.01, *** *P* < 0.001).

differentially regulated in irAOX and wild-type plants (Supplemental Fig. S8B). Similar to *Empoasca* spp.-attacked plants, higher levels of SA in irAOX plants were associated with the lower accumulation of JA-dependent HGL-DTGs (Supplemental Fig. S9). In contrast, the levels of a

typical PAL-dependent phenolic compound, chlorogenic acid (CGA), increased in wild-type and irAOX plants (Supplemental Fig. S9), and this increase was pronounced in plants that lacked AOX gene function.

DISCUSSION

Activation of AOX is an important marker of stress-adaptive cell reprogramming of plants (for review, see Arnholdt-Schmitt et al., 2006). It is also one of the best known examples of mitochondrial retrograde regulation (MRR; for review, see Rhoads and Subbiah, 2007) when nuclear-encoded genes like AOX or antioxidant

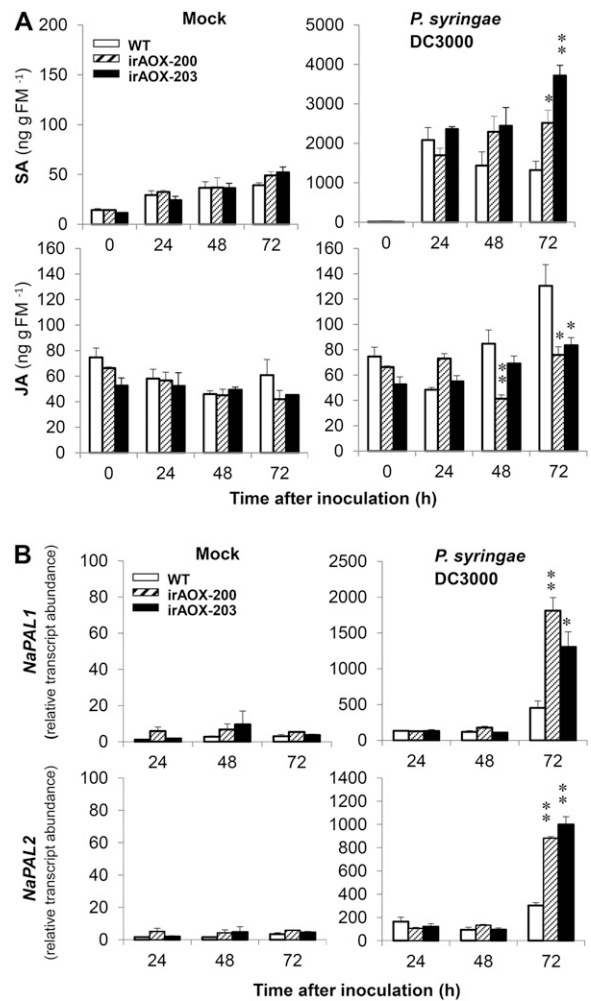


Figure 10. *NaPAL* gene transcript accumulation correlates with increased SA accumulation in *Pst* DC3000-infected irAOX leaves. A, Mean (\pm SE) levels of SA and JA in wild-type and irAOX leaves determined 0, 24, 48, and 72 h after *Pst* DC3000 infection (*n* = 5). Note large differences in scale between mock- and *Pst* DC3000-inoculated SA levels. B, Mean (\pm SE) of *NaPAL* relative transcript abundances quantified with qRT-PCR in mock- and *Pst* DC3000-infected wild-type and two irAOX lines at indicated time points (*n* = 3). Asterisk indicates significant differences between wild-type and irAOX plants at respective time points determined by one-way ANOVA (**P* < 0.05, ***P* < 0.01).

enzymes are induced in response to perturbation of mitochondrial homeostasis. To understand the role of AOX and MRR in defense of *N. attenuata* against biotic stress, we examined NaAOX function in three biotic stress situations using AOX-silenced *N. attenuata* plants. The NaAOX transcript and protein levels significantly increased in all cases; however, the lack of AOX transcripts in irAOX plants showed case-specific modifications of plant responses to biotic stress.

AOX-Modulated Responses to Abiotic Stress

In contrast with the well-known role of AOX in the production of heat in thermogenic plants (Meeuse, 1975), the role of the AOX in nonthermogenic plants remains elusive. Fiorani et al. (2005) observed smaller and larger plants in AOX1a antisense- and sense-transformed Arabidopsis plants, respectively, which were maintained at a low temperature (12°C). In an independent experiment, silencing of the cold-inducible AOX gene did not result in any visible growth phenotype; however, several antioxidant defense genes were strongly up-regulated in the cold-exposed *aox1a* mutant plants, pointing to stronger cold-induced oxidative stress in these plants (Watanabe et al., 2008). Under low nitrogen supply, *aox1a* plants showed slight increase in gene expression of antioxidant enzymes (Watanabe et al., 2010). In *N. tabacum* plants with antisense-targeted AOX gene, higher amounts of H₂O₂ were produced under cold stress (Zhang et al., 2009). From these examples, the control of redox status and ROS levels in plants seems to be a unifying stress-related function of AOX in abiotic stresses. As discussed further, a similar concept can be applied to plants under biotic stress.

Reported Roles of AOX in Plant Resistance to Biotic Stress

To further complement the role of AOX in stress responses, the role of AOX in resistance against two types of herbivores and one pathogen was examined in *N. attenuata* plants. Previously, the role of AOX in response to biotic stress was described in *N. tabacum* 'Xanthi' (nn genotype) plants infected with TMV. Whereas the pretreatment of leaf discs with SA suppressed TMV replication, application of AOX inhibitor salicylhydroxamic acid (SHAM) together with SA counteracted the effect of the hormone on TMV (Chivasa et al., 1997). In addition, application of inhibitors of the Cyt pathway (potassium cyanide [KCN] or antimycin) that elicit AOX transcription via MRR, displayed levels of resistance to TMV that were comparable with SA-induced resistance (Chivasa and Carr, 1998), suggesting a role of SA as potential integrator of mitochondrial function, AOX expression, and MRR. Recently, a nitric oxide-dependent systemic activation of AOX in tomato inoculated with TMV was reported by Fu et al. (2010), showing that AOX is essential for reduced accumulation of viral mRNA and systemic basal resistance to TMV in

tomato plants (Fu et al., 2010). In contrast, the existence of SA-dependent and AOX-independent resistance to viruses in *N. tabacum* plants was proposed by Gilliland et al. (2003). In addition, the overexpression of AOX in transgenic *Nicotiana benthamiana* plants infected with potato virus X increased susceptibility of plants to systemic disease induction and virus accumulation, and AOX modulated SA-induced resistance to potato virus X (Lee et al., 2011).

AOX and Herbivory in *N. attenuata*

Here we show that AOX transcription is efficiently induced by the feeding of a chewing herbivore. However, the suppression of AOX in irAOX plants did not impair resistance of transgenic plants to *M. sexta*, suggesting that these JA-mediated responses are robust and independent of AOX expression. In contrast, the irAOX plants interacting with piercing-sucking insect *Empoasca* spp. (and *Pst* DC3000) showed increased SA levels, suggesting that SA could act as an important intermediate between AOX-regulated processes and JA-mediated defense responses in plants that are attacked by insects associated with minimal tissue damage and/or low JA accumulations.

Even at low concentrations, SA induced transient accumulations of AOX protein and transcripts in cultured cells (Norman et al., 2004), presumably due to the interference with normal mitochondrial function. It has been shown that SA at concentrations as low as 20 μM can rapidly inhibit both ATP synthesis and oxygen uptake in the plant cells; however, the site of SA action has not been clearly elucidated (Xie and Chen, 1999). The effect of SA on respiration by intact cells and isolated mitochondria from *N. tabacum* suspension cell cultures was therefore reexamined by Norman et al. (2004). In these experiments, SA stimulated ADP-limited electron transport at less than 1 mM concentrations, acting as an uncoupler. At higher concentrations, between 1 and 5 mM, SA inhibited respiration in isolated mitochondria by preventing electron flow from the substrate dehydrogenases to the UQ pool, being a potent inhibitor of electron transport. Both the uncoupling and inhibitory effects of SA can explain lower ATP levels in cells observed by Xie and Chen (1999).

Because some of the negative effects of SA were substantially reduced in the presence of strong antioxidant *N*-acetyl-Cys (Xie and Chen, 1999), ROS was likely involved in these responses. Because SA strongly induces AOX (Chivasa et al., 1997; Norman et al., 2004), a self-regulated interaction network involving SA, AOX, and ROS may be proposed in plants. The Arabidopsis *aox1a* mutants showed enhanced ROS production in the roots after direct inhibition of Cyt respiratory pathway by KCN (Umbach et al., 2005). The lack of AOX function moderately increased H₂O₂ levels in TMV-inoculated antisense AOX-targeted *N. tabacum* plants, providing a biologically relevant connection from SA accumulation (typical metabolite induced

by TMV; Yalpani et al., 1991) to AOX-controlled ROS accumulation, similar to that found in *Pst* DC3000-infected irAOX *N. attenuata* plants.

Possible Mechanisms of Accelerated PCD in irAOX Plants

Mitochondria represent one of the most important sources of ROS in plant cells. Recently, it has been shown that mitochondrial complex II of the electron transport chain is a key contributor to localized ROS accumulation during plant stress and defense responses (Gleason et al., 2011). Potato cells treated with β -glucan elicitor displayed dramatic bursts of H_2O_2 , disruption of mitochondrial membrane potential, and PCD when the function of catalase and AOX were simultaneously inhibited by 3-amino-1,2,4-triazol and SHAM, respectively (Mizuno et al., 2005); AOX, therefore, was essential for counteraction of PCD. The application of harpin elicitors strongly induced expression of Arabidopsis AOX1a (Krause and Durner, 2004), further pointing to involvement of AOX in ROS and PCD regulation. In another experiment, harpin treatment rapidly inhibited ATP synthesis in *N. tabacum* cells, similar to the effect of direct SA application (Xie and Chen, 1999), which induced PCD (Xie and Chen, 2000). In addition, *N. tabacum* cells lacking AOX by antisense suppression of the gene showed increased sensitivity to PCD-inducing agents such as H_2O_2 , SA, and protein phosphatase inhibitor cantharidin (Robson and Vanlerberghe, 2002).

At the whole plant level, treatment of Arabidopsis leaves with SA increased the accumulation of H_2O_2 , lipid peroxidation, and oxidative damage to proteins (Rao et al., 1997); however, direct application of H_2O_2 failed to mimic these events. Taking into account the effects of SA on mitochondria, SA is very likely to control mitochondrial ROS in concert with AOX to fine tune the progression of PCD in plants, supported by our findings in *N. attenuata* plants challenged with *Pst* DC3000. The expression of HIN1, a known PCD marker in *N. tabacum* (Takahashi et al., 2004a) increased significantly more in irAOX leaves compared with the wild type after *Pst* infection, supporting our view that AOX functionally counteracts the early development of PCD in pathogen-infected leaves. Recently, Kiba et al. (2008) reported enhanced cell death in *Pst*-infected lettuce (*Lactuca sativa*) leaves after octyl gallate treatment, an effective inhibitor of AOX.

AOX Affecting JA-SA Hormonal Cross Talk

In our experiments with piercing-sucking insects, irAOX plants became more susceptible to *Empoasca* spp. (leafhopper) feeding, both in the glasshouse and under Utah field conditions. The greater susceptibility to piercing-sucking insects correlated with higher accumulation of SA that was associated with a lower content of late-accumulating JA-dependent defense metabolites in irAOX plants. Recently, a detailed analysis of *Empoasca*

spp. host choice was conducted, revealing a key role of JA in initial determination of plant hosts by these insects (Kallenbach et al., 2012); *Empoasca* spp. damage negatively correlated with the ability of these plants to perceive wound-induced JAs (Kallenbach et al., 2012). Similarly, the ectopically higher levels of SA in irAOX plants at later time points could interfere with downstream JA signaling in *N. attenuata* plants, resulting in enhanced feeding of *Empoasca* spp. on these plants. Recently, Leon-Reyes et al. (2010) showed that SA strongly inhibits JA-mediated gene expression in Arabidopsis, leading to a significant down-regulation of typical JA-responsive genes like *PLANT DEFENSIN1.2* and *VEGETATIVE STORAGE PROTEIN2* by mechanisms located downstream of JA biosynthesis. Although we did not find directly reduced JA levels in *Empoasca* spp.-attacked irAOX leaves (associated with moderate AOX-dependent increase of SA), we found significantly reduced JA levels in *Pst*-infected plants (associated with greatly elevated SA levels). Remarkably, lower levels of JA-dependent, defense-related HGLDTGs were identified in both interactions. These data suggest that the amounts as well as ratios between SA and JAs may be important to determine the outcome of stress-modulated JA-SA cross talk in plants.

Insects frequently serve as vectors/hosts for microbial pathogens that cause diseases in plants (Weintraub and Beanland, 2006). Although *Empoasca* spp.-associated *Candidatus* Phytoplasma spp. have not been detected in our insect colony or from insects collected in the field (Kallenbach et al., 2012), other *Empoasca* spp.-transmitted microbes, such as viruses or bacteria, could have been responsible for ectopic accumulation of SA and activation of SA-dependent signaling in AOX-deficient *N. attenuata* plants. Plant antiherbivore defenses countered by pathogenic infections associated with higher levels of SA were recently reported by Thaler et al. (2010). The effect of TMV infection on herbivore performance was tested in the wild type and SA-deficient (NahG) plant backgrounds, showing that SA was required for TMV to increase herbivore vector performance.

Priming and activation of plant immune responses triggered by some beneficial microbes point to an existence of complex interactions mediating both positive and negative roles of microbes in ecological interactions (for review, see Van Wees et al., 2008). It was previously shown that methyl salicylic acid (MeSA) derived from SA is required for systemic acquired resistance (SAR) signal perception in systemic *N. tabacum* tissues (Park et al., 2007). In the same study, it was proposed that a lipid-derived SAR signal could work with (or upstream of) MeSA to activate SAR. Indeed, the local production of MeSA from SA in Arabidopsis by methyltransferase enzyme was shown to be dependent on the *Pst* virulence factor coronatine (functional analog of JA-Ile; Attaran et al., 2009). Because most MeSA was directly emitted into the atmosphere, and only a small amount was retained in the leaves, it was proposed that the phytopathogen is using JA

signaling-dependent, coronatine-mediated volatilization of MeSA from the leaves to attenuate the SA-based defense pathway.

Although antagonistic interactions prevail in examples of JA-SA cross talk, the effects of both signaling pathways need not be mutually exclusive when these responses become temporally or spatially separated. Several JA perception, biosynthetic, and signaling mutants were attenuated in RPM1-mediated systemic immunity (SAR) in *Arabidopsis* plants challenged with an avirulent strain of *Pst*, consistent with a positive role of JA in systemic immunity (Truman et al., 2007). In addition, it was noticed that SA often accumulates 1 d after JA accumulation in natural plant's innate immune response to viruses (Shang et al., 2011), suggesting that JA and SA can act in synergism and confer optimal virus resistance when applied in appropriate concentrations and with a time delay. Indeed, when these changes were simulated by exogenous application of JA and SA, the strong inhibitory efficiency to virus replication was achieved (80%–90%). It will be interesting to see in the future if AOX could be directly involved in these interactions.

CONCLUSION

Although AOX expression is induced by numerous biotic stress factors, the induction of AOX and protection against stress may not always be in a positively linear relationship. *N. attenuata* plants clearly benefited from the activity of AOX and alternative respiration to cope with *Empoasca* spp. attack, and controlled progression of PCD during *Pst* infection. However, they did not gain any clear benefit from inducing AOX after being attacked by *M. sexta* caterpillars. These results prompt further investigations, and the use of additional plant-biotic stress models to unravel additional ecological and physiological roles of alternative respiratory pathways in plants.

MATERIALS AND METHODS

Plant Growth and Treatments

Wild-type *Nicotiana attenuata* plants (22nd inbred generation) seeds, originally collected from a native population in Utah, were used for all experiments, including transformation and generation of transgenic lines. Wild-type plants were transformed with constructs carrying fragments in an inverted repeat orientation of *N. attenuata* AOX1 (AY422688) and lipoxygenase-3 (LOX3), which mediates JA production (Halitschke and Baldwin, 2003). All transformed plants were diploid as determined by flow cytometry and homozygous for a single transgene insertion. Plants from T2 or T3 generations were used in experiments. Seeds were germinated on agar plates supplemented with Gamborg B5 media (Duchefa) according to the procedures described by Krügel et al. (2002). All treatments were performed on rosette stage plants grown in 1-L pots with soil, unless otherwise noted. For W+W and W+OS treatments, leaves were wounded with a pattern wheel and 20 μ L of water, or *Manduca sexta* OS (one-fifth diluted in water) was rubbed into wounds, respectively. For *M. sexta* feeding assays, two freshly hatched neonate larvae were placed on the leaves of each wild-type and irAOX plant. Clip cages were used to restrict movement of larvae on the plant, and samples were collected after 0, 1, 2, and 3 d. Clip-caged leaves from separate plants without larvae were used as controls. For *Empoasca* spp. feeding assays, wild-type and

transgenic lines were placed into a glass container (110 \times 50 \times 80 cm) with *Empoasca* spp. reared on *Cucurbita moschata*, *Cucurbita maxima* var Goldnugget, and *Cucurbita pepo* plants, and *Empoasca* spp. were allowed to choose the host plants. The estimated colony size at the time of experiment was 800 to 1000 *Empoasca* spp. in the glass box. Samples from *Empoasca* spp.-infested plants were collected after 0, 4, 8, and 12 d. A set of plants growing next to the box with *Empoasca* spp. were used to collect control samples. Bacterial strain of *Pseudomonas syringae* pv *tomato* (*Pst*) DC3000 was cultivated on Luria-Bertani plates supported with agar containing 25 mg/L rifampicin and 5 mg/L tetracycline at 28°C. Bacterial growth assays and inoculation of the leaves were carried out essentially as described in Rayapuram et al. (2008).

In the field, 15-d-old seedlings were transferred into previously hydrated 50-mm peat pellets (Jiffy 703; <http://www.jiffypot.com>) and grown in shade tents for 2 weeks to gradually adjust the plants to the high sun and low relative humidity conditions of the Great Basin Desert. Three to four weeks later, when plants were in the early rosette stage of growth, size-matched wild-type/irAOX-203 plant pairs were transplanted into an irrigated field plot (at a distance of 1.5 m between the pairs) in the 2008 growing season at the Lytle Ranch Preserve near Santa Clara, Utah. The release of transgenics was carried under Animal and Plant Health Inspection Service notification 06–242–3r and the seeds were imported under 07–341–101n.

Generation and Characterization of NaAOX-Silenced Plants (ir-AOX)

A 510-bp fragment of the complementary DNA (cDNA) sequence of the *NaAOX1* gene (position 338–848 in AY422688) was inserted into the pSOL3 transformation vector (Bubner et al., 2006) as an inverted-repeat construct to generate pSOL3AOX vector (Supplemental Fig. S3A). *N. attenuata* wild-type plants were transformed with pSOL3AOX vector using an *Agrobacterium tumefaciens*-mediated transformation procedure previously described by Krügel et al. (2002). The gene for hygromycin resistance (*hptII*) allowed selecting hygromycin-resistant transgenic plants on the agar plates supplemented with 35 mg/L hygromycin (Krügel et al., 2002). Southern-blot hybridization of genomic DNA from independently transformed T1 generation plants and from the wild-type line was carried out according to a standard protocol, using 32 P-labeled PCR fragment of the *hptII* gene as a probe. Independent transgenic lines harboring a single copy of the transgene (Supplemental Fig. S3B) were further screened for homozygosity after germination on hygromycin-containing GB5 media. Two independently transformed single-insert homozygous lines, 200 and 203, strongly suppressed in their *NaAOX* transcript accumulation, were selected for further experiments.

Expression Analysis by qRT-PCR

Total RNA was extracted from approximately 100 mg of leaf tissue using TRIZOL reagent (Invitrogen; <http://www.invitrogen.com>), and total RNA was treated with RQ1 RNase-free DNase to remove all DNA contaminants (Promega; <http://www.promega.com>). RNA samples were diluted to a final concentration 0.5 μ g/ μ L, and 1 μ g of total RNA was used for cDNA synthesis with oligo(dT) primer (Fermentas; <http://www.fermentas.com>) and Super-script II reverse transcriptase (Invitrogen; <http://www.invitrogen.com>) following a standard protocol. qRT-PCR assays were performed on a Stratagene Mx3005P real-time PCR system (<http://www.stratagene.com>) using qPCR kit for SYBR Green I and qPCR Core kit for Taqman assays (Eurogentec GmbH; <http://www.eurogentec.com>). To determine *NaAOX* gene transcript levels in irAOX lines, gene specific primers were designed outside the region used in the ir-silencing construct. Gene-specific primers were designed with Primer3 software (<http://frodo.wi.mit.edu/primer3>). Relative gene expression was calculated from linear standard curves prepared by serial dilutions of a specific cDNA standard sample. An actin housekeeping gene from *N. attenuata* (EU273278) was used as endogenous reference to normalize the gene expression. The primers, Taqman probe sequences, and primer sequences for SYBR Green-based qRT-PCR are described in Supplemental Table S1.

AOX Protein Determination by Western Blot

Leaves were ground to a fine powder in liquid nitrogen, and 100 μ L of 2 \times Laemmli buffer with 2% (v/v) β -mercaptoethanol was added to 150 mg of tissue before protein extractions. The samples were centrifuged for 20 min at 16,100g, and protein concentration in the cleared supernatants was determined by the Bradford reagent (Sigma; <http://www.sigmaldrich.com>). The aliquots

(25 μg) of protein were boiled for 3 min in Eppendorf tubes and separated on 10% SDS-PAGE gel. Proteins from the gel were electroblotted onto a polyvinylidene difluoride membrane (GE Healthcare Life Sciences; <http://www.gelifesciences.com>) in Tris-Glyc buffer and 20% (v/v) methanol. AOX protein was immunodetected using a commercial polyclonal antibody against *Arabidopsis thaliana* AOX (Agrisera; <http://www.agrisera.com>) at a dilution of 1:1000 and WesternBreeze immunodetection kit (Invitrogen; <http://www.invitrogen.com>). The manufacturer's instructions were followed except for the following modifications: membranes were blocked overnight at 4°C, and washing steps were prolonged to 10 min.

Measurement of Respiration in *N. attenuata* Leaves

The plants were placed in the dark for 15 min before the start of respiration measurements. Leaf discs were excised by an 8-mm-diameter cork borer from the leaves and placed in the plastic syringe with assay buffer (20 mM HEPES, 0.2 mM CaCl_2 , pH 7.2; Simons et al., 1999) supplied with inhibitors or without inhibitors for determination of total respiration. The leaf discs were briefly infiltrated by creating a partial vacuum in the syringe and incubated in the dark for 15 min. Four infiltrated discs (approximately 80 mg fresh mass) were transferred into a 4-mL glass vial filled with fresh O_2 -saturated assay buffer (2 mL) equipped with a miniaturized Clark-type oxygen electrode (Oxygen Microsensor, Unisense). After initial equilibration of the electrode for several minutes, O_2 consumption was continuously measured in the dark for 2 to 3 min and recorded using Sensor Trace Basic 3.1.1 software (Unisense) in 10-s intervals. Total respiration rates (V_{TOTAL}) were determined as leaf disc O_2 uptake ($\mu\text{mol min}^{-1} \text{g fresh mass}^{-1}$) in the assay buffer without inhibitors. The cyanide-sensitive Cyt-dependent respiration (V_{CIT}) was determined in the assay buffer containing 1 mM KCN and calculated as $V_{\text{TOTAL}} - V_{\text{KCN}}$. Finally, cyanide-insensitive but SHAM-sensitive alternative respiration (V_{ALT}) was determined after addition of 5 mM SHAM to 1 mM KCN-containing buffer and calculated as difference $V_{\text{KCN}} - V_{\text{KCN+SHAM}}$ (Furuhashi et al., 1989).

Phytohormone Analysis

Harvested leaves were immediately frozen in liquid nitrogen and stored at -80°C until analysis. Phytohormones SA, JA, and JA-Ile were extracted following the procedure described in Wu et al. (2007). In brief, 150 mg of leaf material was extracted with 1 mL of ethyl acetate spiked with 200 ng D_4 -SA, $^{13}\text{C}_2$ -JA, and $^{13}\text{C}_6$ -JA-Ile as internal standards in FastPrep tubes containing 0.9 g of FastPrep Matrix (Sili GmbH; <http://www.sigmund-lindner.com>). The tissues were homogenized in 2000 GENO/GRINDER homogenizer (SPEX CertiPrep; <http://www.spexcsp.com>) for 2 min, and samples were centrifuged at 13,000g for 20 min at 4°C. The supernatants were transferred to clean 2-mL Eppendorf tubes, and each pellet was reextracted with 1 mL of ethyl acetate and centrifuged. Combined supernatants were dried in a vacuum concentrator to near dryness (Eppendorf; <http://www.eppendorf.com>) before resuspending the samples in 0.5 mL of 70% methanol (v/v). Ten microliters of extract was subjected to reverse-phase HPLC coupled to tandem mass spectrometry using the 1200LC LC/MS-MS-MS system (Varian; <http://www.varianinc.com>) according to the procedure described in Wu et al. (2007). The levels of each phytohormone were calculated based on the peak area of the labeled internal standards and fresh mass of the sample.

Analysis of Secondary Metabolites

Secondary metabolites were analyzed by HPLC coupled to diode array detector as described in Kaur et al. (2010). Approximately 100 mg of leaf material was extracted with 1 mL of extraction buffer containing 40% (v/v) methanol and 0.5% (v/v) acetic acid. After centrifugation, the supernatants were collected and injected into an Agilent 1100 series HPLC (<http://www.chem.agilent.com>) equipped with ODS Inertsil C18 column (3 μm , 150 \times 4.6 mm i.d.) that was protected by a Phenomenex Security Guard C18 precolumn (Phenomenex; <http://www.phenomenex.com>). Nicotine, rutin, and CGA standards were used to construct corresponding calibration curves. CP and dicaffeoylpermidine contents were calculated on the basis of CGA calibration that showed nearly identical UV-absorption profile.

Determination of Cell Death

Trypan blue staining specific to dead cells with permeabilized cytoplasmic membranes was carried out as described in Koch et al. (1991). Electrolyte

leakage was measured as described in Pike et al. (1998) using a conductivity meter (Mettler; <http://us.mt.com/>). Eight discs (0.785 cm^2 each) were punched from the treated leaves using a cork borer and placed in 15-mL Falcon tubes (BD Biosciences; <http://www.bdbiosciences.com>) together with 10 mL of sterile distilled water. Samples were incubated for 4 h under slow rotation at 20°C, and the conductivity of resulting water solutions was measured by conductivity meter.

H_2O_2 Visualization and Determinations

DAB staining was performed on the leaves inoculated with *Pst* DC3000 or mock solutions as described by Thordal-Christensen et al. (1997) with some modifications. Leaves with petioles were excised from the plants at each point in time after bacteria infiltration and supplied with 1 mg/mL DAB solution through the petioles until a brown precipitate was observed in the leaf blades (5 h). Leaves were destained in boiling ethanol (96%) for 10 min and fixed in 3:1:1 ethanol/lactic acid/glycerol solution. To determine endogenous concentrations of H_2O_2 , liquid nitrogen-stored leaves were ground in liquid nitrogen, and 100 mg of tissue powders were extracted in 200 μL of 25 mM HCl supplemented with 50 mg of activated charcoal. After 1 to 2 min vortexing, samples were kept on ice for 10 min and centrifuged at 12,000g for 20 min at 4°C. Cleared supernatants were transferred to clean tubes, and H_2O_2 concentrations were determined using Amplex red hydrogen peroxide/peroxidase assay kit (Invitrogen; <http://www.invitrogen.com>). H_2O_2 was used to construct calibration curves. Prior to each measurement, 10 μL of each extract was neutralized with 90 μL of 1 \times reaction buffer, and 50 μL of neutralized extract was loaded on a 96-well Nunc multiwell plate (Thermo Scientific; <http://www.nuncbrand.com>). Next, 50 μL of reaction buffer was dispensed into each well to initiate the reaction. Samples were incubated for 30 min at room temperature before measurement of fluorescent intensities at Excitation/Emission 530/590 nm in an Infinite 200 multimode reader (Tecan Group Ltd.; <http://www.tecan.com>).

Supplemental Data

The following materials are available in the online version of this article.

Supplemental Figure S1. AOX genes from *N. attenuata* are highly homologous to AOX1 a gene from *Arabidopsis*.

Supplemental Figure S2. NaAOX proteins increase in response to simulated herbivory, feeding of *M. sexta* caterpillars, *Empoasca* spp. attack, and *Pst* DC3000 infection in *N. attenuata*.

Supplemental Figure S3. Structure of plant transformation vector pSO-L3AOX used for silencing of AOX genes in *N. attenuata* and characterization of irAOX transgenic lines.

Supplemental Figure S4. Functional characterization of irAOX lines.

Supplemental Figure S5. irAOX WOS- and herbivory-induced plants have salicylate levels and H_2O_2 levels comparable to wild-type plants.

Supplemental Figure S6. Exposure to *M. sexta* feeding does not change a majority of the secondary metabolite profiles in irAOX plants compared with the wild type.

Supplemental Figure S7. Silencing of NaLOX3 compromises defense of *N. attenuata* against *Empoasca* spp.

Supplemental Figure S8. Multiplication of *Pst* DC3000 is slightly suppressed in irAOX plants and *NaICS* transcript levels are not differentially regulated in wild-type and irAOX plants infected with *Pst* DC3000.

Supplemental Figure S9. Secondary metabolites levels are altered in irAOX plants relative to the wild type after *Pst* DC3000 infection.

Supplemental Table S1. Real-time PCR primers and probes.

ACKNOWLEDGMENTS

We thank S. Sudakaran from the Department of Insect Symbiosis, Max Planck Institute for Chemical Ecology for help with measurement of plant respiration, and members of the Department of Molecular Ecology, Max Planck Institute for Chemical Ecology, S. Kutschbach and A. Wissgott for

help with plant transformation, A. Weber and A. Schünzel for growing the plants in the glasshouse, D. Kessler and Jesse Colangelo Lillis for help with field experiments, A. Kessler for providing *Empoasca* spp. field photo, and Brigham Young University for use of their field station at the Lytle Ranch Preserve.

Received May 22, 2012; accepted September 3, 2012; published September 7, 2012.

LITERATURE CITED

- Ament K, Kant MR, Sabelis MW, Haring MA, Schuurink RC (2004) Jasmonic acid is a key regulator of spider mite-induced volatile terpenoid and methyl salicylate emission in tomato. *Plant Physiol* **135**: 2025–2037
- Arnholdt-Schmitt B, Costa JH, De Melo DF (2006) AOX—a functional marker for efficient cell reprogramming under stress? *Trends Plant Sci* **11**: 281–287
- Attaran E, Zeier TE, Griebel T, Zeier J (2009) Methyl salicylate production and jasmonate signaling are not essential for systemic acquired resistance in *Arabidopsis*. *Plant Cell* **21**: 954–971
- Backus EA, Serrano MS, Ranger CM (2005) Mechanisms of hopperburn: an overview of insect taxonomy, behavior, and physiology. *Annu Rev Entomol* **50**: 125–151
- Baldwin IT (2001) An ecologically motivated analysis of plant-herbivore interactions in native tobacco. *Plant Physiol* **127**: 1449–1458
- Bartoli CG, Gomez F, Gergoff G, Guimét JJ, Puntarulo S (2005) Up-regulation of the mitochondrial alternative oxidase pathway enhances photosynthetic electron transport under drought conditions. *J Exp Bot* **56**: 1269–1276
- Bassard JE, Ullmann P, Bernier F, Werck-Reichhart D (2010) Phenolamides: bridging polyamines to the phenolic metabolism. *Phytochemistry* **71**: 1808–1824
- Bolton MD (2009) Primary metabolism and plant defense—fuel for the fire. *Mol Plant Microbe Interact* **22**: 487–497
- Bubner B, Gase K, Berger B, Link D, Baldwin IT (2006) Occurrence of tetraploidy in *Nicotiana attenuata* plants after *Agrobacterium*-mediated transformation is genotype specific but independent of polysomaty of explant tissue. *Plant Cell Rep* **25**: 668–675
- Chivasa S, Carr JP (1998) Cyanide restores N gene-mediated resistance to tobacco mosaic virus in transgenic tobacco expressing salicylic acid hydroxylase. *Plant Cell* **10**: 1489–1498
- Chivasa S, Murphy AM, Naylor M, Carr JP (1997) Salicylic acid interferes with tobacco mosaic virus replication via a novel salicylhydroxamic acid-sensitive mechanism. *Plant Cell* **9**: 547–557
- Costa JH, Jolivet Y, Hasenfratz-Sauder MP, Orellano EG, Da Guia Silva Lima M, Dizengremel P, Fernandes de Melo D (2007) Alternative oxidase regulation in roots of *Vigna unguiculata* cultivars differing in drought/salt tolerance. *J Plant Physiol* **164**: 718–727
- De Vos M, Van Oosten VR, Jander G, Dicke M, Pieterse CM (2007) Plants under attack: multiple interactions with insects and microbes. *Plant Signal Behav* **2**: 527–529
- Dinakar C, Raghavendra AS, Padmasree K (2010) Importance of AOX pathway in optimizing photosynthesis under high light stress: role of pyruvate and malate in activating AOX. *Physiol Plant* **139**: 13–26
- Feng HQ, Wang YF, Li HY, Wang RF, Sun K, Jia LY (2010a) Salt stress-induced expression of rice AOX1a is mediated through an accumulation of hydrogen peroxide. *Biologia* **65**: 868–873
- Fiorani F, Umbach AL, Siedow JN (2005) The alternative oxidase of plant mitochondria is involved in the acclimation of shoot growth at low temperature. A study of *Arabidopsis* AOX1a transgenic plants. *Plant Physiol* **139**: 1795–1805
- Fu LJ, Shi K, Gu M, Zhou YH, Dong DK, Liang WS, Song FM, Yu JQ (2010) Systemic induction and role of mitochondrial alternative oxidase and nitric oxide in a compatible tomato-tobacco mosaic virus interaction. *Mol Plant Microbe Interact* **23**: 39–48
- Furuhashi K, Hosaka Y, Kabasawa T (1989) Increases in cyanide-resistant respiration and ethanol fermentation in rice callus cells with increases in the supply of sucrose. *Plant Cell Physiol* **30**: 459–461
- Gleason C, Huang SB, Thatcher LF, Foley RC, Anderson CR, Carroll AJ, Millar AH, Singh KB (2011) Mitochondrial complex II has a key role in mitochondrial-derived reactive oxygen species influence on plant stress gene regulation and defense. *Proc Natl Acad Sci USA* **108**: 10768–10773
- Gilliland A, Singh DP, Hayward JM, Moore CA, Murphy AM, York CJ, Slatore J, Carr JP (2003) Genetic modification of alternative respiration has differential effects on antimycin A-induced versus salicylic acid-induced resistance to tobacco mosaic virus. *Plant Physiol* **132**: 1518–1528
- Halitschke R, Baldwin IT (2003) Antisense LOX expression increases herbivore performance by decreasing defense responses and inhibiting growth-related transcriptional reorganization in *Nicotiana attenuata*. *Plant J* **36**: 794–807
- Hanqing F, Kun S, Mingquan L, Hongyu L, Xin L, Yan L, Yifeng W (2010) The expression, function and regulation of mitochondrial alternative oxidase under biotic stresses. *Mol Plant Pathol* **11**: 429–440
- Heiling S, Schuman MC, Schoettner M, Mukerjee P, Berger B, Schneider B, Jassbi AR, Baldwin IT (2010) Jasmonate and ppHsystemin regulate key malonylation steps in the biosynthesis of 17-hydroxygeranylinalool diterpene glycosides, an abundant and effective direct defense against herbivores in *Nicotiana attenuata*. *Plant Cell* **22**: 273–292
- Henry MF, Nyns ED (1975) Cyanide-insensitive respiration. An alternative mitochondrial pathway. *Subcell Biochem* **4**: 1–65
- Hettenhausen C, Baldwin IT, Wu J (2012) Silencing MPK4 in *Nicotiana attenuata* enhances photosynthesis and seed production but compromises abscisic acid-induced stomatal closure and guard cell-mediated resistance to *Pseudomonas syringae* pv *tomato* DC3000. *Plant Physiol* **158**: 759–776
- Hiser C, McIntosh L (1990) Alternative oxidase of potato is an integral membrane protein synthesized de novo during aging of tuber slices. *Plant Physiol* **93**: 312–318
- Jassbi AR, Gase K, Hettenhausen C, Schmidt A, Baldwin IT (2008) Silencing geranylgeranyl diphosphate synthase in *Nicotiana attenuata* dramatically impairs resistance to tobacco hornworm. *Plant Physiol* **146**: 974–986
- Kallenbach M, Bonaventure G, Gilardoni PA, Wissgott A, Baldwin IT (2012) *Empoasca* leafhoppers attack wild tobacco plants in a jasmonate-dependent manner and identify jasmonate mutants in natural populations. *Proc Natl Acad Sci USA* **109**: E1548–E1557
- Kaur H, Heinzl N, Schöttner M, Baldwin IT, Gális I (2010) R2R3-NaMYB8 regulates the accumulation of phenylpropanoid-polyamine conjugates, which are essential for local and systemic defense against insect herbivores in *Nicotiana attenuata*. *Plant Physiol* **152**: 1731–1747
- Kempema LA, Cui XP, Holzer FM, Walling LL (2007) *Arabidopsis* transcriptome changes in response to phloem-feeding silverleaf whitefly nymphs. Similarities and distinctions in responses to aphids. *Plant Physiol* **143**: 849–865
- Kessler A, Halitschke R, Baldwin IT (2004) Silencing the jasmonate cascade: induced plant defenses and insect populations. *Science* **305**: 665–668
- Kiba A, Lee KY, Ohnishi K, Hikichi Y (2008) Comparative expression analysis of genes induced during development of bacterial rot and induction of hypersensitive cell death in lettuce. *J Plant Physiol* **165**: 1757–1773
- Koch E, Larak M, Ellendorff F (1991) Comparative studies on in vitro reactivity of fresh and cryopreserved pig lymphocytes. *Cryobiology* **28**: 405–412
- Krause M, Durner J (2004) Harpin inactivates mitochondria in *Arabidopsis* suspension cells. *Mol Plant Microbe Interact* **17**: 131–139
- Krügel T, Lim M, Gase K, Halitschke R, Baldwin IT (2002) *Agrobacterium*-mediated transformation of *Nicotiana attenuata*, a model ecological expression system. *Chemoecology* **12**: 177–183
- Lee WS, Fu SF, Verchot-Lubicz J, Carr JP (2011) Genetic modification of alternative respiration in *Nicotiana benthamiana* affects basal and salicylic acid-induced resistance to potato virus X. *BMC Plant Biol* **11**: 41
- Lennon AM, Neuenschwander UH, Ribas-Carbo M, Giles L, Ryals JA, Siedow JN (1997) The effects of salicylic acid and tobacco mosaic virus infection on the alternative oxidase of tobacco. *Plant Physiol* **115**: 783–791
- Leon-Reyes A, Van der Does D, De Lange ES, Delker C, Westernack C, Van Wees SC, Ritsema T, Pieterse CM (2010) Salicylate-mediated suppression of jasmonate-responsive gene expression in *Arabidopsis* is targeted downstream of the jasmonate biosynthesis pathway. *Planta* **232**: 1423–1432
- Liao YWK, Shi K, Fu LJ, Zhang S, Li X, Dong DK, Jiang YP, Zhou YH, Xia XJ, Liang WS, et al (2012) The reduction of reactive oxygen species formation by mitochondrial alternative respiration in tomato basal defense against TMV infection. *Planta* **235**: 225–238
- Maffei ME, Mithöfer A, Boland W (2007) Before gene expression: early events in plant-insect interaction. *Trends Plant Sci* **12**: 310–316
- Maxwell DP, Wang Y, McIntosh L (1999) The alternative oxidase lowers mitochondrial reactive oxygen production in plant cells. *Proc Natl Acad Sci USA* **96**: 8271–8276

- McDonald AE** (2008) Alternative oxidase: an inter-kingdom perspective on the function and regulation of this broadly distributed 'cyanide-resistant' terminal oxidase. *Funct Plant Biol* **35**: 535–552
- Meeuse BJD** (1975) Thermogenic respiration in aroids. *Annu Rev Plant Physiol* **26**: 117–126
- Metlen KL, Aschehoug ET, Callaway RM** (2009) Plant behavioural ecology: dynamic plasticity in secondary metabolites. *Plant Cell Environ* **32**: 641–653
- Millar AH, Whelan J, Soole KL, Day DA** (2011) Organization and regulation of mitochondrial respiration in plants. *Annu Rev Plant Biol* **62**: 79–104
- Mizuno M, Tada Y, Uchii K, Kawakami S, Mayama S** (2005) Catalase and alternative oxidase cooperatively regulate programmed cell death induced by beta-glucan elicitor in potato suspension cultures. *Planta* **220**: 849–853
- Moore AL, Bonner WD Jr, Rich PR** (1978) The determination of the proton-motive force during cyanide-insensitive respiration in plant mitochondria. *Arch Biochem Biophys* **186**: 298–306
- Mozoruk J, Hunnicutt LE, Cave RD, Hunter WB, Bausher MG** (2006) Profiling transcriptional changes in *Citrus sinensis* (L.) Osbeck challenged by herbivory from the xylem-feeding leafhopper *Homalodisca coagulata* (Say) by cDNA microarray analysis. *Plant Sci* **170**: 1068–1080
- Norman C, Howell KA, Millar AH, Whelan JM, Day DA** (2004) Salicylic acid is an uncoupler and inhibitor of mitochondrial electron transport. *Plant Physiol* **134**: 492–501
- Ordog SH, Higgins VJ, Vanlerberghe GC** (2002) Mitochondrial alternative oxidase is not a critical component of plant viral resistance but may play a role in the hypersensitive response. *Plant Physiol* **129**: 1858–1865
- Park SW, Kaimoyo E, Kumar D, Mosher S, Klessig DF** (2007) Methyl salicylate is a critical mobile signal for plant systemic acquired resistance. *Science* **318**: 113–116
- Pike SM, Adam AL, Pu XA, Hoyos ME, Laby R, Beer SV, Novacky A** (1998) Effects of *Erwinia amylovora* harpin on tobacco leaf cell membranes are related to leaf necrosis and electrolyte leakage and distinct from perturbations caused by inoculated *E. amylovora*. *Physiol Mol Plant Pathol* **53**: 39–60
- Popov VN, Eprintsev AT, Maltseva EV** (2011) Activation of genes encoding mitochondrial proteins involved in alternative and uncoupled respiration of tomato plants treated with low temperature and reactive oxygen species. *Russ J Plant Physiol* **58**: 914–920
- Rao MV, Paliyath G, Ormrod DP, Murr DP, Watkins CB** (1997) Influence of salicylic acid on H₂O₂ production, oxidative stress, and H₂O₂-metabolizing enzymes. Salicylic acid-mediated oxidative damage requires H₂O₂. *Plant Physiol* **115**: 137–149
- Raskin I, Ehmann A, Melander WR, Meeuse BJD** (1987) Salicylic acid: a natural inducer of heat production in *arum* lilies. *Science* **237**: 1601–1602
- Rayapuram C, Wu J, Haas C, Baldwin IT** (2008) PR-13/Thionin but not PR-1 mediates bacterial resistance in *Nicotiana attenuata* in nature, and neither influences herbivore resistance. *Mol Plant Microbe Interact* **21**: 988–1000
- Rhoads DM, Subbaiah CC** (2007) Mitochondrial retrograde regulation in plants. *Mitochondrion* **7**: 177–194
- Rhoads DM, Umbach AL, Subbaiah CC, Siedow JN** (2006) Mitochondrial reactive oxygen species. Contribution to oxidative stress and inter-organellar signaling. *Plant Physiol* **141**: 357–366
- Robson CA, Vanlerberghe GC** (2002) Transgenic plant cells lacking mitochondrial alternative oxidase have increased susceptibility to mitochondria-dependent and -independent pathways of programmed cell death. *Plant Physiol* **129**: 1908–1920
- Ruiz OH, Gonzalez A, Almeida AJ, Tamayo D, Garcia AM, Restrepo A, McEwen JG** (2011) Alternative oxidase mediates pathogen resistance in *Paracoccidioides brasiliensis* infection. *PLoS Negl Trop Dis* **5**: e1353
- Seymour RS** (1997) Plants that warm themselves. *Sci Am* **276**: 104–109
- Shang J, Xi DH, Xu F, Wang SD, Cao S, Xu MY, Zhao PP, Wang JH, Jia SD, Zhang ZW, et al** (2011) A broad-spectrum, efficient and non-transgenic approach to control plant viruses by application of salicylic acid and jasmonic acid. *Planta* **233**: 299–308
- Simons BH, Millenaar FF, Mulder L, Van Loon LC, Lambers H** (1999) Enhanced expression and activation of the alternative oxidase during infection of *Arabidopsis* with *Pseudomonas syringae* pv *tomato*. *Plant Physiol* **120**: 529–538
- Stephuhn A, Gase K, Krock B, Halitschke R, Baldwin IT** (2004) Nicotine's defensive function in nature. *PLoS Biol* **2**: E217
- Takahashi Y, Berberich T, Yamashita K, Uehara Y, Miyazaki A, Kusano T** (2004a) Identification of tobacco *HINI* and two closely related genes as spermine-responsive genes and their differential expression during the Tobacco mosaic virus-induced hypersensitive response and during leaf- and flower-senescence. *Plant Mol Biol* **54**: 613–622
- Takahashi Y, Uehara Y, Berberich T, Ito A, Saitoh H, Miyazaki A, Terauchi R, Kusano T** (2004b) A subset of hypersensitive response marker genes, including *HSR203j*, is the downstream target of a spermine signal transduction pathway in tobacco. *Plant J* **40**: 586–595
- Thaler JS, Agrawal AA, Halitschke R** (2010) Salicylate-mediated interactions between pathogens and herbivores. *Ecology* **91**: 1075–1082
- Thordal-Christensen H, Zhang ZG, Wei YD, Collinge DB** (1997) Subcellular localization of H₂O₂ in plants. H₂O₂ accumulation in papillae and hypersensitive response during the barley-powdery mildew interaction. *Plant J* **11**: 1187–1194
- Torres MA, Dangl JL, Jones JD** (2002) *Arabidopsis* gp91phox homologues AtrbohD and AtrbohF are required for accumulation of reactive oxygen intermediates in the plant defense response. *Proc Natl Acad Sci USA* **99**: 517–522
- Truman W, Bennett MH, Kubigsteltig I, Turnbull C, Grant M** (2007) *Arabidopsis* systemic immunity uses conserved defense signaling pathways and is mediated by jasmonates. *Proc Natl Acad Sci USA* **104**: 1075–1080
- Umbach AL, Fiorani F, Siedow JN** (2005) Characterization of transformed *Arabidopsis* with altered alternative oxidase levels and analysis of effects on reactive oxygen species in tissue. *Plant Physiol* **139**: 1806–1820
- Vanlerberghe GC, McIntosh L** (1992) Lower growth temperature increases alternative pathway capacity and alternative oxidase protein in tobacco. *Plant Physiol* **100**: 115–119
- Van Wees SC, Van der Ent S, Pieterse CM** (2008) Plant immune responses triggered by beneficial microbes. *Curr Opin Plant Biol* **11**: 443–448
- Vidal G, Ribas-Carbo M, Garmier M, Dubertret G, Rasmussen AG, Mathieu C, Foyer CH, De Paepe R** (2007) Lack of respiratory chain complex I impairs alternative oxidase engagement and modulates redox signaling during elicitor-induced cell death in tobacco. *Plant Cell* **19**: 640–655
- Vlot AC, Dempsey DA, Klessig DF** (2009) Salicylic acid, a multifaceted hormone to combat disease. *Annu Rev Phytopathol* **47**: 177–206
- Wang J, Rajakulendran N, Amirsadeghi S, Vanlerberghe GC** (2011) Impact of mitochondrial alternative oxidase expression on the response of *Nicotiana tabacum* to cold temperature. *Physiol Plant* **142**: 339–351
- Watanabe CK, Hachiya T, Takahara K, Kawai-Yamada M, Uchimiyama H, Uesono Y, Terashima I, Noguchi K** (2010) Effects of AOX1a deficiency on plant growth, gene expression of respiratory components and metabolic profile under low-nitrogen stress in *Arabidopsis thaliana*. *Plant Cell Physiol* **51**: 810–822
- Watanabe CK, Hachiya T, Terashima I, Noguchi K** (2008) The lack of alternative oxidase at low temperature leads to a disruption of the balance in carbon and nitrogen metabolism, and to an up-regulation of antioxidant defence systems in *Arabidopsis thaliana* leaves. *Plant Cell Environ* **31**: 1190–1202
- Weintraub PG, Beanland L** (2006) Insect vectors of phytoplasmas. *Annu Rev Entomol* **51**: 91–111
- Wu J, Baldwin IT** (2010) New insights into plant responses to the attack from insect herbivores. *Annu Rev Genet* **44**: 1–24
- Wu J, Hettenhausen C, Meldau S, Baldwin IT** (2007) Herbivory rapidly activates MAPK signaling in attacked and unattacked leaf regions but not between leaves of *Nicotiana attenuata*. *Plant Cell* **19**: 1096–1122
- Xie Z, Chen Z** (1999) Salicylic acid induces rapid inhibition of mitochondrial electron transport and oxidative phosphorylation in tobacco cells. *Plant Physiol* **120**: 217–226
- Xie Z, Chen Z** (2000) Harpin-induced hypersensitive cell death is associated with altered mitochondrial functions in tobacco cells. *Mol Plant Microbe Interact* **13**: 183–190
- Yalpani N, Silverman P, Wilson TM, Kleier DA, Raskin I** (1991) Salicylic acid is a systemic signal and an inducer of pathogenesis-related proteins in virus-infected tobacco. *Plant Cell* **3**: 809–818
- Zhang Y, Xi D, Wang J, Zhu D, Guo X** (2009) Functional analysis reveals effects of tobacco alternative oxidase gene (NtAOX1a) on regulation of defence responses against abiotic and biotic stresses. *Biosci Rep* **29**: 375–383
- Zhang DW, Xu F, Zhang ZW, Chen YE, Du JB, Jia SD, Yuan S, Lin HH** (2010) Effects of light on cyanide-resistant respiration and alternative oxidase function in *Arabidopsis* seedlings. *Plant Cell Environ* **33**: 2121–2131
- Zhu L, Li YM, Li L, Yang JH, Zhang MF** (2011) Ethylene is involved in leafy mustard systemic resistance to turnip mosaic virus infection through the mitochondrial alternative oxidase pathway. *Physiol Mol Plant Pathol* **76**: 166–172